Role of K/Bi disorder in the electronic structure of β-$K_2Bi_8Se_{13}$

Khang Hoang,[1] Aleksandra Tomic,[2] S. D. Mahanti,[2,*] Theodora Kyratsi,[3]
Duck-Young Chung,[4] S. H. Tessmer,[2] and Mercouri G. Kanatzidis[4,5]
[1]*Materials Department, University of California, Santa Barbara, California 93106, USA*
[2]*Department of Physics and Astronomy, Michigan State University, East Lansing, Michigan 48824, USA*
[3]*Department of Mechanical and Manufacturing Engineering, University of Cyprus, Nicosia 1678, Cyprus*
[4]*Materials Science Division, Argonne National Laboratory, Argonne, Illinois 60439, USA*
[5]*Department of Chemistry, Northwestern University, Evanston, Illinois 60208, USA*
(Received 30 March 2009; revised manuscript received 29 June 2009; published 15 September 2009)

We have carried out tunneling spectroscopy and first-principles studies for β-$K_2Bi_8Se_{13}$, a promising thermoelectric material with partially disordered mixed K/Bi sites. The tunneling data, obtained with a scanning tunneling microscope (STM), show that the system is a semiconductor with a band gap of ~0.4 eV and band-tail states near the valence-band top and the conduction-band bottom. First-principles calculations, on the other hand, show that β-$K_2Bi_8Se_{13}$ can be semimetallic or semiconducting depending on the arrangements of the K and Bi atoms in the mixed sites. The electronic structure of β-$K_2Bi_8Se_{13}$ near the band-gap region is largely determined by unbonded Se p states and states associated with strained bonds which are present due to K/Bi disorder and by the Bi p-Se p hybridization which tends to drive the system toward metallicity. Among the different K/Bi arrangements investigated, we have identified a structural model (quasidisordered structure) that is able to satisfactorily reproduce the atomic and electronic structures of β-$K_2Bi_8Se_{13}$; i.e., the local composition in the mixed channels as observed experimentally and the band gap and tails as seen in the STM measurements. We argue that transport properties of β-$K_2Bi_8Se_{13}$ can be qualitatively understood in terms of the electronic structure obtained in calculations using the above structural model.

DOI: 10.1103/PhysRevB.80.125112 PACS number(s): 71.20.Nr, 71.23.An, 72.15.Jf

I. INTRODUCTION

In the last several decades, significant efforts have been focused on finding efficient materials for thermoelectric applications. Many different classes of materials have been explored; some examples are complex chalcogenides, skutterudites, half-Heusler alloys, metal oxides, and intermetallic clathrates.[1] Among the complex chalcogenides, β-$K_2Bi_8Se_{13}$, a narrow band gap and partially disordered semiconductor, has been found to be a promising thermoelectric material at room temperature. The compound exhibits very low thermal conductivity (~1.3 W/m K) and relatively high power factor (~12 μW/cm K^2).[2]

β-$K_2Bi_8Se_{13}$ crystallizes in the monoclinic $P2_1/m$ space group with $a=17.492(3)$ Å, $b=4.205(1)$ Å, $c=18.461(4)$ Å, $\beta=90.49(2)°$. This structure possesses a three-dimensional architecture made up of Bi_2Te_3-, NaCl-, and CdI_2-type infinite rod-shaped blocks. Alternately, it can be described as having one-dimensional channels running along the crystallographic b axis each containing K, Bi, Se, or K and Bi atoms. There are one inequivalent channel (per unit cell) fully occupied with K atoms denoted as K(2) and two inequivalent channels denoted as K(1)/Bi(9) and Bi(8)/K(3) containing mixtures of K and Bi atoms. The Bi(8)/K(3) channel contains 62% Bi and 38% K, whereas the K(1)/Bi(9) channel contains 62% K and 38% Bi.[2] The enhanced thermoelectric property of this system is believed to arise from the unusually low thermal conductivity resulting from a large unit cell with low symmetry, the weakly bound K^+ ions, and the disorder associated with the mixed-occupancy K/Bi channels.

Low thermal conductivity is only a part of the thermoelectric physics of this system. In order to understand the physical reason behind the observed large power factor one has to look at the electronic structure of this complex material. It is well known that transport and optical properties of semiconductors depend sensitively on the nature of the electronic states near the band gap.[3] Thus, it is necessary to understand the nature of these states in β-$K_2Bi_8Se_{13}$ and how they are affected by the K/Bi disorder. In this work, we carry out detailed studies of the electronic structure of β-$K_2Bi_8Se_{13}$ using both tunneling spectroscopy measurements and first-principles calculations. The tunneling measurements were acquired with a cryogenic scanning tunneling microscope (STM), allowing us to investigate the electronic structure of the system in the neighborhood of the chemical potential at low temperature. These measurements provide an important experimental reference which allows for a critical evaluation of different theoretical structural models that take into account the observed disorder in the system.

First-principles calculations have become an important tool to investigate different types of structural disorder and how they impact the electronic properties. Although in principle the disorder effects can be studied using realistic models for disorder, in practice one makes use of supercells that model different configurations for the K/Bi mixed sites in β-$K_2Bi_8Se_{13}$ to make such calculations feasible. This investigation serves two purposes, one is to understand the interplay between atomic and electronic structures and the role played by the K/Bi disorder, and two is to identify model(s) that best reproduces the atomic and electronic structures of β-$K_2Bi_8Se_{13}$ as seen in experiments.

Earlier first-principles studies carried out by Bilc *et al.*[4] using supercell models have provided limited information on the atomic and electronic structures of β-$K_2Bi_8Se_{13}$. As we

will discuss in Sec. III, the models proposed in Ref. 4 do not correctly reproduce the observed local composition of the mixed channels and hence the fine details of the electronic structure of the system. In this paper, we propose a structural model that better describes the atomic and electronic structures of β-$K_2Bi_8Se_{13}$. Some of the supercell models proposed earlier by Bilc *et al.* will also be reinvestigated and comparison between different models will be made.

The arrangement of this paper is as follows: in Sec. II, we provide some details on the β-$K_2Bi_8Se_{13}$ sample preparation and results of the tunneling measurements. Several supercell models designed for first-principles calculations and the calculational details are presented in Sec. III. In Sec. IV, we discuss our results of the energetics, atomic and electronic structures for different models of β-$K_2Bi_8Se_{13}$. We conclude this paper with a summary in Sec. V.

II. STM MEASUREMENTS

The β-$K_2Bi_8Se_{13}$ samples used in this study were grown by reacting stoichiometric combination of elemental K, Bi, and Se. All manipulations were carried out under a dry nitrogen atmosphere in a Vacuum Atmospheres Dri-Laboratory glove-box. A mixture of 0.282 g of K, 6.021 g of elemental Bi, and 3.697 g of elemental Se was loaded into silica tube, which was subsequently flame-sealed at a residual pressure of $<10^{-4}$ Torr. The mixture was heated to 850 °C over 12 h and kept there for 1 h, followed by cooling to 450 °C and kept there for 48 h, and cooling to 50 °C at a rate of −15 °C/h. We find that the electronic grade of the material is very high; all samples for measurements discussed here were selected randomly.[5,6] There is no composition variation or segregation as concluded from x-ray diffraction and energy dispersive x-ray analysis measurements (within the techniques' accuracy). Regarding thermoelectric properties, we have measured the Seebeck coefficient on a sample from the same ingot as the STM measurement, shown below; we find a value of -120 ± 15 μV/K at 300 K, where the uncertainty is due to limitations of the measurement method. Seebeck measurements on samples from different ingots agree with this value to within the uncertainty.

Transport measurements indicate that β-$K_2Bi_8Se_{13}$ and related samples are at relatively high doping level as prepared, and that they remain good conductors at low temperature.[7] As discussed in Ref. 7, the system is well described by a finite-gap semiconductor model, with the addition of a significant concentration of charge carriers originating from the disorder. Further investigation of this issue is the major focus of the present paper.

For the STM measurements, the crystals were cleaved on a laboratory bench top with a razor blade parallel to *b*-axis, and then quickly placed in a high-vacuum environment of a cryogenic STM system, similar to the system described in Ref. 8. The tunneling signals we observed were robust and stable; moreover, high-quality reproducible tunneling spectroscopy curves were observed, as described below. Hence we believe that surface contamination and oxide were minimal. However, attempts to obtain atomically resolved images at room-temperature and low-temperature were unsuccessful.

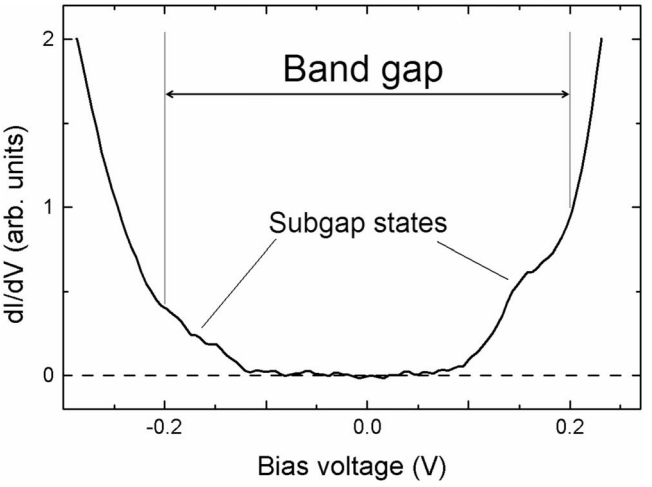

FIG. 1. Local density of states of β-$K_2Bi_8Se_{13}$ as obtained by STM spectroscopic measurements at 1.6 K. The labels on the horizontal axis give the voltage applied to the sample, relative to the tip (there is no shift or effective zero voltage introduced). The dI/dV curve shows two basic features: a gap and band tails, which we label as subgap states. The gap size has been estimated to be approximately ~0.4 eV, by linear extrapolation of the dI/dV curve before it changes slope at the subgap states. The assigned size of the gap is then the approximate voltage between the two intercepts of extrapolated lines with the zero dI/dV baseline.

Tunneling spectroscopy measurements on a cleaved surface of β-$K_2Bi_8Se_{13}$ were performed at 1.6 K for various positions of the probing tip above the surface of the sample. Sweeping the bias voltage V over a range of ± 300 mV, we have measured tunneling current I as a function of the ramped voltage. Differentiation of $I(V)$ data with respect to V gives the thermally broadened local density of states. The measurements for a given tip position were repeated 100 times, and averaged, in order to improve signal-to-noise ratio.

A representative measurement of the density of states of β-$K_2Bi_8Se_{13}$ is shown in Fig. 1. Because atomic resolution was not achieved, we do not know which part of the unit cell was probed. However, data were acquired at several tip positions, all of which show nearly identical spectroscopic features. Hence we do not have evidence of significant spectroscopic variations from atom to atom. The thermal smearing of the density of states is 3.5 k_BT, where k_B is the Boltzmann constant and T is temperature; this results in a voltage smearing of 5×10^{-4} V, which is negligible over the displayed range of data. The data clearly indicate the presence of a band gap. The magnitude of the observed gap is ~0.4 eV.[9] As can be seen in Fig. 1, the spectroscopy data also shows the presence of band-tail states (subgap states), seen as finite density of states in the gap region both near the top of the valence band and near the bottom of the conduction band. Possible explanations of the origin of these states are surface states, defects, and/or the presence of disorder. In the following, we will show that the band tails can indeed be understood in terms of the K/Bi disorder that exists in the system.

III. THEORETICAL MODELING

A. Supercell models

As discussed earlier, β-$K_2Bi_8Se_{13}$ contains channels with mixed K/Bi occupancy, perhaps in a disordered fashion. Although mixed occupancy as well as disorder can be treated using, for example, coherent potential approximation,[10,11] they cannot be handled in a realistic fashion by our current first-principles calculations based on density functional theory (DFT). We have therefore used different ordered configurations for the K(1)/Bi(9) and Bi(8)/K(3) channels, using large supercells, to model the mixed sites. This approach can help us understand how the arrangement of the different atoms in the mixed channels and their local geometry affect the electronic structure of β-$K_2Bi_8Se_{13}$, particularly near the band-gap region. Based on our understanding of the interplay between atomic and electronic structures, we can then identify a supercell model with minimum size that can mimic the crystal structure of partially disordered β-$K_2Bi_8Se_{13}$.

Several supercell models have been proposed earlier by Bilc *et al.*[4] to understand the electronic structure of β-$K_2Bi_8Se_{13}$. Among the proposed configurations for the K(1)/Bi(9) and Bi(8)/K(3) mixed channels there was one with extreme occupancy, hereafter called model M1, that contains 100% Bi on the Bi(8)/K(3) site and 100% K on the K(1)/Bi(9) site. This model (which has 46 atoms/cell) clearly does not reproduce the observed local composition of the mixed channels, i.e., 62% Bi and 38% K on the Bi(8)/K(3) site and 62% K and 38% Bi on the K(1)/Bi(9) site. In order to incorporate the mixed occupancy, a $(1\times2\times1)$ supercell with 92 atoms was also proposed.[4] This model (M2) requires doubling of the unit cell with respect to the unit cell given by the experiment (average occupancy picture). It has K and Bi atoms alternatively occupying the mixed sites along the channels. Each mixed channel has 50% Bi and 50% K. In Ref. 4, models M1 and M2 were referred to as "configuration I" and "configuration III," respectively.

As we will show later, these two models do not satisfactorily reproduce the electronic structure of β-$K_2Bi_8Se_{13}$ as seen in our spectroscopy measurements. We, therefore, introduce a new structural model (M3) that can take into account the local composition in the K(1)/Bi(9) and Bi(8)/K(3) channels more accurately. This model requires unit cell tripling along the *b* axis with respect to the unit cell given by experiment, resulting in a $(1\times3\times1)$ supercell with 138 atoms. The mixed channels, K(1)/Bi(9) and Bi(8)/K(3), are modeled by repeating (K-Bi-K) unit (67% K and 33% Bi) and (Bi-K-Bi) unit (67% Bi and 33% K), respectively, along the *b* axis.

B. Calculational details

Structural optimization, total energy and electronic structure calculations were performed within the DFT formalism, using the generalized-gradient approximation (GGA) (Ref. 12) and the projector-augmented wave (PAW) (Refs. 13 and 14) method as implemented in the VASP code.[15–17] We used the standard PAW potentials in the VASP database. Scalar relativistic effects (mass-velocity and Darwin terms) and spin-orbit interaction (SOI) were included, except in ionic optimization where only scalar relativistic effects were taken into account. Each calculation begins with volume optimization and ionic position relaxations of a chosen structure, the relaxed structure was then used to calculate energy and single-particle electronic density of states (DOS).

For the calculations of models M1, M2, and M3, we used $3\times14\times3$ (35 **k** points in the irreducible Brillouin zone), $3\times7\times3$ (32 **k** points), and $3\times5\times3$ (23 **k** points) Monkhorst-Pack[18] **k**-point meshes, respectively, for the self-consistent run to calculate charge densities. More **k** points ($\sim$50% larger) were used to produce high-quality electronic DOSs. In all the calculations, the energy cutoff was set to 220 eV and the convergence was assumed when the total energy between cycles was less than 10^{-4} eV. A choice of denser **k**-point meshes and/or larger energy cutoff does not change the physics of what we are presenting.

IV. RESULTS AND DISCUSSION

A. Atomic relaxations and energetics

We find remarkable changes in the local geometry of β-$K_2Bi_8Se_{13}$ in all the three models. The optimized volumes of the supercells are larger compared to the experimental value by $\sim$3%. This is expected since it is known that DFT-GGA tends to overestimate the lattice constants.[19] Regarding internal relaxations, the displacements from the initial positions are largest for the Bi atoms in the mixed channels, i.e., Bi(8) and Bi(9), and for their neighboring Se atoms. This is a result of the strong hybridization between trivalent cation (Bi)*p* and divalent anion (Se)*p* states as seen in many chalcogenides,[20,21] and the initial positions of the Bi atoms in the mixed channels being far from equilibrium. Note that, in the initial structures (models M1, M2, and M3), K and Bi are treated equally in the mixed channels, i.e., without taking into account the fact that they bond differently to the neighboring Se atoms. The large geometric relaxations also result in large (internal) relaxation energies, measured as the difference between the total energy of the fully relaxed (volume, cell shape, and positions of ions) supercell and that of the partially relaxed (only volume optimization) supercell; −802, −722, and −720 meV/f.u. for M1, M2, and M3, respectively, where f.u.=$K_2Bi_8Se_{13}$.

Figure 2 shows the relaxed structure of β-$K_2Bi_8Se_{13}$ in model M1 where the mixed sites are occupied by 100% K or 100% Bi. The most notable feature in this structure is the presence of onefold coordinated Se atoms, Se(9). Se(9) channels are sandwiched between K(1) and K(2) channels; Se(9) atoms only bond to their nearest neighbor Bi(3) atoms with the Se(9)-Bi(3) distance being 2.62 Å. This relaxation pattern is clearly caused by the deficit of Bi in the local environment of the Se(9) atoms. Besides having Se(9) as the nearest neighbor, Bi(3) in model M1 has two Se(10) atoms as the second nearest neighbors with the bond lengths being 2.79 Å.

Figure 3 shows the relaxed structure of β-$K_2Bi_8Se_{13}$ in model M2. Unlike M1, there is no onefold coordinated Se atoms in M2 which has 50% K and 50% Bi in the mixed channels. Both Se(9) and Se(4) are twofold coordinated. Bi(8) and Bi(9) in the mixed channels relax appreciably to-

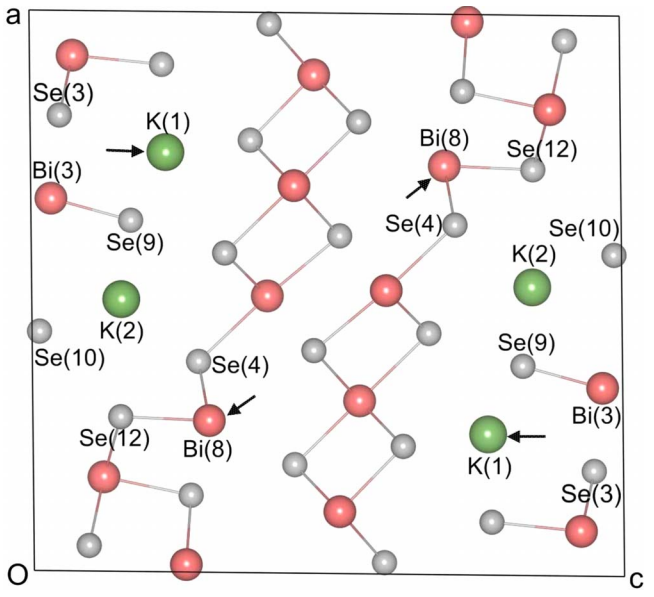

FIG. 2. (Color online) Relaxed structure of β-$K_2Bi_8Se_{13}$ in model M1 (46 atoms/cell). The view is along the *b* axis. Potassium is represented by large (green) spheres, bismuth is medium (red), and selenium is small (gray). This model contains 100% K and 100% Bi, respectively, on the K(1)/Bi(9) and Bi(8)/K(3) mixed sites (marked by arrows). After relaxations, Se(9) is onefold coordinated, with the Se(9)-Bi(3) bond length being 2.62 Å. Bi(8) has one Se(12) atom as its nearest neighbor (bond length: 2.81 Å) and two Se(4) atoms as its second-nearest neighbors (bond lengths: 2.84 Å). Only bonds with bond length smaller than 3.1 Å are shown.

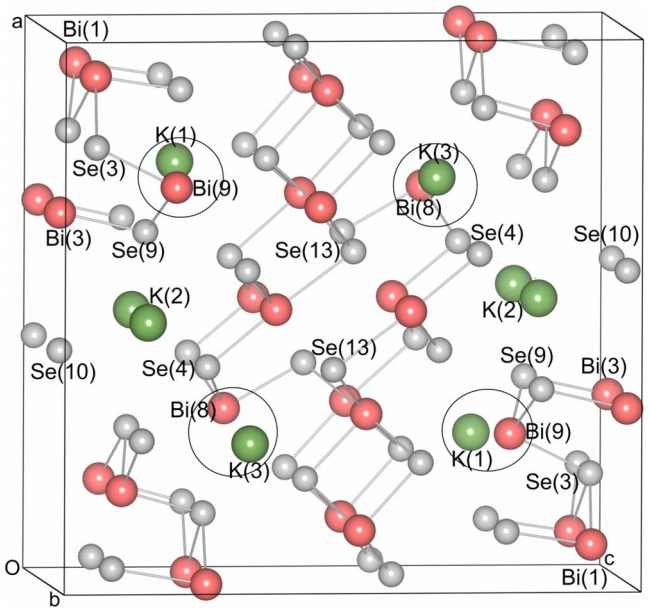

FIG. 3. (Color online) Relaxed structure of β-$K_2Bi_8Se_{13}$ in model M2 (92 atoms/cell). The viewing direction is approximately parallel to the *b* axis. Potassium is represented by large (green) spheres, bismuth is medium (red), and selenium is small (gray). This model requires unit cell doubling along the *b* axis with respect to the unit cell given by experiment. The mixed sites, K(1)/Bi(9) and Bi(8)/K(3) [marked by circles], are modeled by K-Bi-… and Bi-K-… channels, respectively, along the *b* axis; both channels have 50% K and 50% Bi. After relaxations, the Bi(9) atom in the K(1)/Bi(9) channel moves closer and forms bonds with two Se(9) atoms (bond lengths: 2.70 and 2.73 Å) and one Se(3) atom (bond length: 2.90 Å). The Bi(9) atom in the Bi(8)/K(3) channel, on the other hand, moves closer and forms bonds with two Se(9) atoms (bond lengths: 2.70 and 2.76 Å) and one Se(13) atom (bond length: 2.94 Å). Only bonds with bond length smaller than 3.1 Å are shown.

ward their respective neighboring Se atoms, Se(4) and Se(9), respectively.

Model M3, on the other hand, has one third of the Se(9) atoms that are onefold coordinated, two-third of the atoms in the Se(9) channels are twofold coordinated; see Fig. 4. This is because of the deficit of Bi in the K(1)/Bi(9) mixed chains where one has only 33% Bi. In this model, we also find that Bi(8) and Bi(9) strongly relax toward, respectively, Se(4) and Se(9). As we will discuss below, the onefold coordinated Se atoms seen in some of these models play a very important role in determining the electronic structure of the system near the band gap.

Energetically, model M2 has the lowest energy, lower than models M1 and M3 by 299 and 92 meV/f.u., respectively. One can understand this trend in terms of the presence (or absence) of undercoordinated Se atoms. In M1 there is a channel containing Se atoms in which each Se atom has only one Bi atom as a neighbor to bond and stabilize its *p* orbitals. In M2 each Se atom is bonded to two Bi atoms whereas in M3 there is a mixture of one- and twofold coordinated Se atoms. These differences in bonding and their impact on the electronic structure of β-$K_2Bi_8Se_{13}$ will be discussed in detail later. What is interesting and surprising is that although on energetic grounds the ordered 50-50 mixture of K and Bi channels (model M2) is most favorable, it is likely that the presence of quasidisordered 33–67 mixture (model M3) makes that system kinetically more favorable, given the experimentally observed structure.

B. Electronic structure

Figure 5 shows the total DOS of β-$K_2Bi_8Se_{13}$ in model M1 focusing on the electronic structure near the band-gap region. Model M1 shows semimetallic feature, consistent with results reported by Bilc *et al.*[4] In the earlier calculations, where only partial internal relaxations were performed, the band structure did not appear to change appreciably due to internal relaxation. In the present calculations, we have carried out full internal relaxation and have monitored the DOS in the neighborhood of the Fermi level. We find that atomic relaxations reduce the DOS in the region near the Fermi level considerably by pushing some states toward lower and some states toward higher energies. An analysis of the wave functions shows that the region below and near the Fermi level is predominantly Se(9)*p* states, which are unbonded, and a small contribution from the Se(10)*p* states; whereas the region above and near the Fermi level is predominantly hybridized Bi(8)*p* and Se(4)*p* states.

The above results can be understood in terms of the observed relaxed structure of β-$K_2Bi_8Se_{13}$ in model M1 (see also Fig. 2) where Se(9) is onefold coordinated and Bi(8) and Se(4) are the nearest neighbors of one another. The electronic

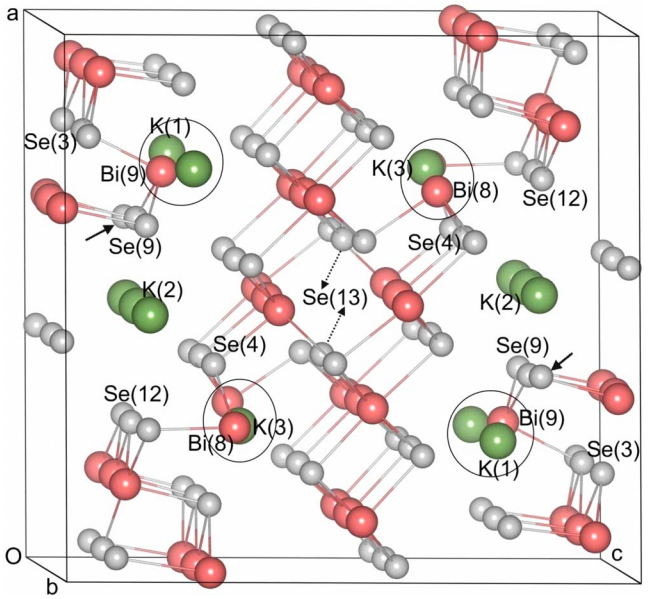

FIG. 4. (Color online) Relaxed structure of β-$K_2Bi_8Se_{13}$ in model M3 (138 atoms/cell). The viewing direction is approximately parallel to the *b* axis. Potassium is represented by large (green) spheres, bismuth is medium (red), and selenium is small (gray). This model requires unit cell tripling along the *b*-axis with respect to the unit cell given by experiment. The mixed sites, K(1)/Bi(9) and Bi(8)/K(3) [marked by circles], are modeled by K-Bi-K-… (67% K and 33% Bi) and Bi-K-Bi-… (67% Bi and 33% K) channels, respectively, along the *b* axis. After relaxations, the Bi(9) atom in the K(1)/Bi(9) channel moves closer and forms bonds with two Se(9) atoms (bond lengths: 2.69 and 2.71 Å) and one Se(3) atom (bond length: 2.89 Å). There are two Bi(8) atoms in the K(3)/Bi(8) channel which relax toward different directions. One Bi(8) atom moves closer and forms bonds with two Se(4) atoms (bond lengths: 2.77 and 2.80 Å) and one Se(12) atom (bond length: 2.81 Å). The other Bi(8) atom moves closer and forms bonds with two Se(4) atoms (bond lengths: 2.72 and 2.83 Å) and one Se(13) atom (bond length: 2.87 Å). One-third of the Se(9) atoms is onefold coordinated [marked by arrows] because of the deficit of Bi in the K(1)/Bi(9) channels. Only bonds with bond length smaller than 3.1 Å are shown.

structure near the band-gap region in model M1 is, therefore, determined by the onefold coordinated Se(9) atoms and the hybridization between Bi(8)*p* and Se(4)*p* states. The latter introduces hybridized *p* states into the band-gap region from the conduction-band bottom and reduces (or even closes) the band gap. This is consistent with the observations in many chalcogenides where the hybridization between trivalent cation *p* states and divalent anion *p* states tends to drive the system toward metallicity.[20,21]

Figure 6 shows the total DOS of β-$K_2Bi_8Se_{13}$ in model M2. In this model, both the valence- and conduction-band edges are sharp for both the relaxed and the unrelaxed structures. This indicates that the electronic states coming from Se(4), Se(9), Bi(8), and Bi(9) are completely stabilized, consistent with our analysis of the relaxed structure of model M2 and also the fact that this model gives the lowest energy. An analysis of the wave functions indeed shows that the top of the valence band is predominantly Se(10)*p* states with

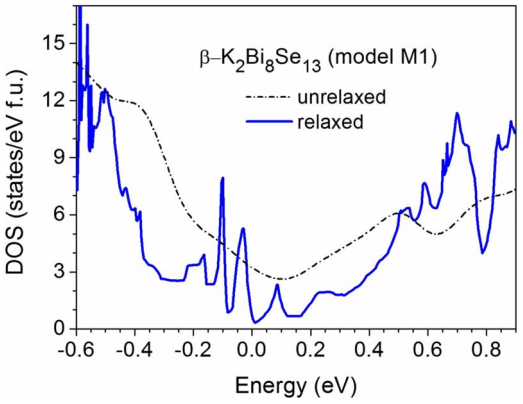

FIG. 5. (Color online) Total DOS of β-$K_2Bi_8Se_{13}$ (model M1) obtained in calculations using unrelaxed (dash dotted curve) and relaxed (solid curve) structures; SOI was included. The Fermi level (at 0 eV) is set to the highest occupied state; f.u.=$K_2Bi_8Se_{13}$. This model shows semimetallic character.

very small contribution from hybridized states of Se(9)*p* and Bi *p*; the conduction-band bottom consists predominantly of Bi(1)*p* states with small contribution from Bi(3)*p* states. There are no unbonded Se *p* states (as seen in model M1) and the hybridized states coming from Bi(9)*p*-Se(9)*p* and Bi(8)*p*-Se(4)*p* hybridizations are stabilized by, respectively, the monovalent cation K(1) and K(3) in the K(1)/Bi(9) and Bi(8)/K(3) mixed channels. The relaxed structure gives a band gap of ~0.52 eV, slightly larger than the unrelaxed one (by 0.10 eV). The calculated band gap in the unrelaxed structure is in good agreement with the earlier results of Bilc *et al.*[4] (~0.41 eV), where only the supercell volume was optimized. This indicates that the internal atomic relaxations are important and can significantly affect the electronic structure of the system near the band gap. We note that SOI has strong effects on the electronic structure of β-$K_2Bi_8Se_{13}$, reducing the band gap by a significant amount (from 0.75 to 0.52 eV for model M2).

The total DOS of β-$K_2Bi_8Se_{13}$ for model M3, which gives a more accurate partial occupancy of the K/Bi channels, is

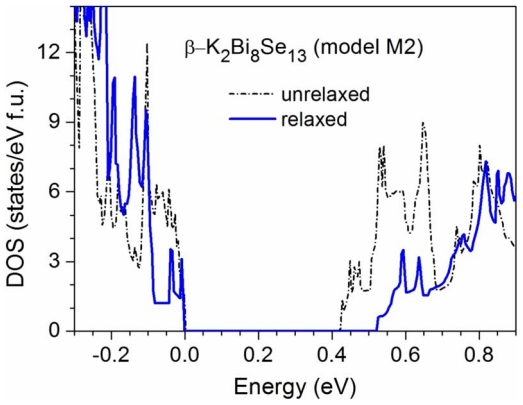

FIG. 6. (Color online) Total DOS of β-$K_2Bi_8Se_{13}$ (model M2) obtained in calculations using unrelaxed (dash dotted curve) and relaxed (solid curve) structures; SOI was included. The Fermi level (at 0 eV) is set to the highest occupied state; f.u.=$K_2Bi_8Se_{13}$. The band gap is ~0.52 eV (relaxed) and the band edges are sharp (no band tails) in this model.

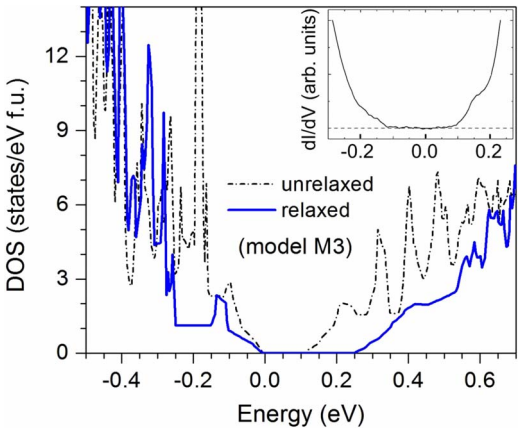

FIG. 7. (Color online) Total DOS of β-$K_2Bi_8Se_{13}$ (model M3) obtained in calculations using unrelaxed (dash dotted curve) and relaxed (solid curve) structures; SOI was included. The Fermi level is set to the highest occupied state; f.u.=$K_2Bi_8Se_{13}$. There are band-tail states in this model formed by the unbonded states associated with the onefold coordinated Se(9) atoms, the hybridized Bi p-Se p states near the mixed channels, and those coming from strained bonds associated with a wide range of Bi and Se atoms. The local density of states of β-$K_2Bi_8Se_{13}$ obtained by STM spectroscopic measurements (Fig. 1) is shown in the inset for comparison.

shown in Fig. 7. This model gives a semiconducting gap of ~0.25 eV, much smaller than seen in M2. However there is a different way to interpret the DOS for this model, namely a band gap of ~0.4 eV (>0.25 eV) with a large band-tail density of states both below the conduction band and above the valence band. An examination of the wave functions shows that the states associated with the valence band tail are predominantly Se(10)p states with contribution from the p states of the onefold coordinated Se(9) atoms and a small contribution from the Bi(3)p states. The conduction band tail states are primarily Bi(1)p states and contributions from a wide range of other Bi and Se atoms including the hybridized Bi p-Se p states that are not fully stabilized by the monovalent K because of the deficit of K atoms in the Bi(8)/K(3) channels. This is shown clearly in Fig. 8, where we plot the partial charge densities associated with the valence-band top and the conduction-band bottom of β-$K_2Bi_8Se_{13}$.

Clearly, the unbonded p states of the onefold coordinated Se(9) atoms, which account for one third of the total number of atoms in the Se(9) channels, play a crucial role in forming the valence band-tail states in model M3. There are possibly other contributions from the strained bonds associated with a variety of Bi and Se atoms to the valence band tail (and to the conduction band tail), given the complexities of the relaxed structure where atoms in the neighboring region of the mixed sites are strongly perturbed from their average positions. We note that studies on defective crystalline Si and amorphous Si by Pan *et al.*[22] also showed that band tails existed in these systems and there were correlations between the band-tail states and the long and short bonds in the lattice.

C. Comparison with experiment

Let us now make comparison between the results obtained in first-principles studies and those from experiments. The computed DOS for model M3 and the results of STM measurements for β-$K_2Bi_8Se_{13}$ show remarkable similarities (see Fig. 7). The gap between the subgap states is ~0.2 eV whereas the calculated band gap is ~0.25 eV. The values of

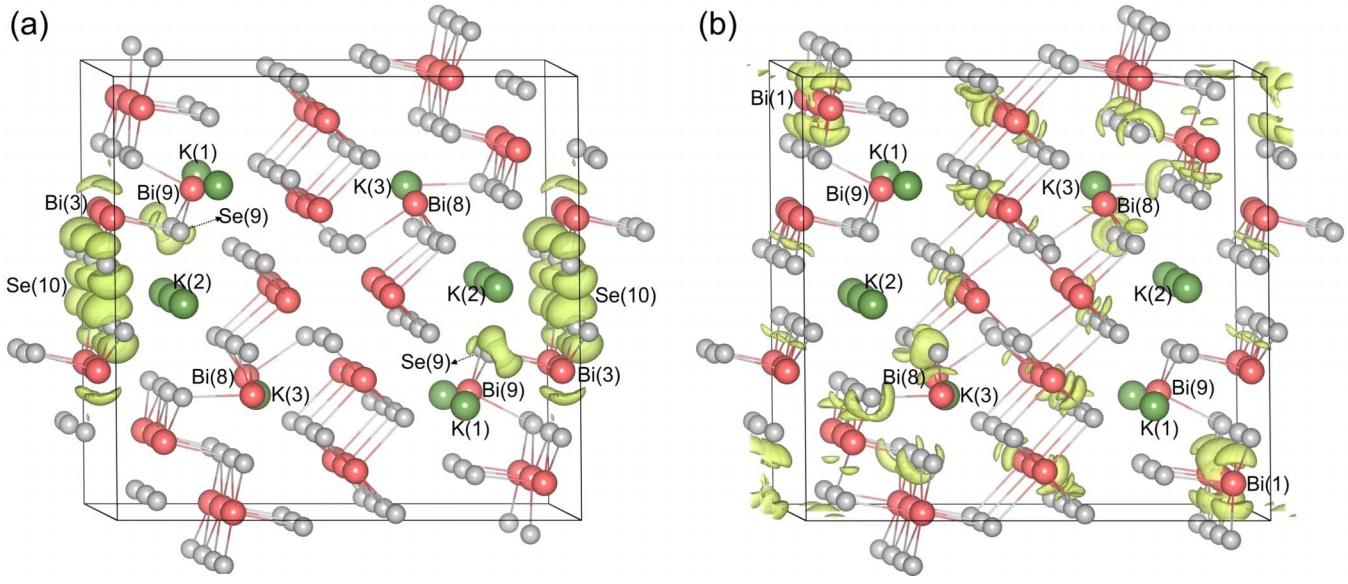

FIG. 8. (Color online) Partial charge density associated with (a) the valence-band top (in the energy range −0.2 to 0 eV) and (b) the conduction-band bottom (in the energy range +0.2 to +0.4 eV) as illustrated by electron clouds around the atoms; the energy ranges are with respect to the total DOS of β-$K_2Bi_8Se_{13}$ (model M3) shown in Fig. 7. The isosurface corresponds to (charge density) × (supercell volume)=10.5 in (a) and 1.5 in (b). Potassium is represented by large (green) spheres, bismuth is medium (red), and selenium is small (gray). In (a), the visualized charge density is predominantly Se(10) with contribution from the onefold coordinated Se(9) atoms and a small contribution from Bi(3), whereas in (b) it is Bi(1) and contributions from a wide range of other Bi and Se atoms.

the band gap between the valence-band maximum and the conduction-band minimum (disregarding the subgap or band-tail states) in spectroscopy measurements and in theoretical calculations are comparable and are estimated to be of ~0.4 eV.

The overall agreement between the density of states obtained for model M3 and the STM measurements appears to be quite good; however, one should consider this agreement with some caution because of the usual band gap underestimation by DFT-GGA,[19] and the close agreement is perhaps fortuitous. What is important is that the DFT calculations give a physical picture of the electronic states near the top of the valence band and the bottom of the conduction band, referred to as the "subgap" states in the description of our STM results. These states are present only when the K/Bi mixed channels have stoichiometry consistent with experiment.

Although there may be limitations associated with DFT-GGA calculations and the simplicity of the model to capture the mixed occupancy along K/Bi channels, the ability of model M3 to reproduce band-tail states as seen in the spectroscopy measurements provides strong validation for this model, making it an excellent candidate that can be used for further theoretical studies and analyses of partially disordered β-$K_2Bi_8Se_{13}$, such as in structural analysis and in first-principles calculations of the transport properties. Among the three models that we have presented, model M3 is also closest to the experimental crystal structure of β-$K_2Bi_8Se_{13}$ in terms of the local composition of the mixed sites. Careful PDF measurements[23] can validate some of our theoretical predictions in terms of different bond lengths due to internal relaxations.

Finally, our results for the electronic structure of β-$K_2Bi_8Se_{13}$ are consistent with measured transport properties of β-$K_2Bi_8Se_{13}$ (and its alloys with the Sb analog),[7] where the experimental data were successfully interpreted by using a narrow band-gap semiconductor model. In addition, the band tails observed in first-principles calculations (using model M3) and in the spectroscopy measurements may explain why β-$K_2Bi_8Se_{13}$ has higher electrical conductivity without much loss of thermoelectric power, compared to its allotropic kin α-$K_2Bi_8Se_{13}$ which does not contain channels with mixed occupancy.[2,24]

V. SUMMARY

In summary, the electronic density of states in the neighborhood of the Fermi energy of β-$K_2Bi_8Se_{13}$, a partially disordered narrow band-gap semiconductor with mixed occupancy on two K/Bi sites, was studied using scanning tunneling spectroscopy. The STM spectroscopic data showed that this material is a narrow band-gap semiconductor with a band gap of ~0.4 eV. The spectroscopy measurements also revealed the presence of band tail (subgap) states.

First-principles calculations using different supercell models (M1, M2, and M3) showed that β-$K_2Bi_8Se_{13}$ can either be a semimetal or a semiconductor depending on how the K and Bi atoms are arranged in the mixed-occupancy channels. Among these models, M3 was found to satisfactorily reproduce the atomic and electronic structures of partially disordered β-$K_2Bi_8Se_{13}$, including the local composition in the mixed channels as observed experimentally and the band gap and band tails as seen in the spectroscopy measurements. The transport properties of β-$K_2Bi_8Se_{13}$ can be qualitatively understood in terms of the electronic structure obtained in our studies.

ACKNOWLEDGMENTS

This work was supported in part by the Office of Naval Research and NSF Grant No. 0305461, and made use of the computing facilities of Michigan State University High Performance Computing Center.

*Corresponding author; mahanti@pa.msu.edu

[1] G. S. Nolas, J. Poon, and M. G. Kanatzidis, MRS Bull. **31**, 199 (2006), and references therein.

[2] D. Y. Chung, K. S. Choi, L. Iordanidis, J. L. Schindler, P. W. Brazis, C. R. Kannewurf, B. Chen, S. Hu, C. Uher, and M. G. Kanatzidis, Chem. Mater. **9**, 3060 (1997).

[3] G. D. Mahan and J. O. Sofo, Proc. Natl. Acad. Sci. U.S.A. **93**, 7436 (1996).

[4] D. I. Bilc, S. D. Mahanti, T. Kyratsi, D.-Y. Chung, M. G. Kanatzidis, and P. Larson, Phys. Rev. B **71**, 085116 (2005).

[5] Th. Kyratsi, J. S. Dyck, W. Chen, D.-Y. Chung, C. Uher, K. M. Paraskevopoulos, and M. G. Kanatzidis, J. Appl. Phys. **92**, 965 (2002).

[6] Th. Kyratsi, D.-Y. Chung, and M. G. Kanatzidis, J. Alloys Compd. **338**, 36 (2002).

[7] Th. Kyratsi, E. Hatzikraniotis, K. M. Paraskevopoulos, C. D. Malliakas, J. S. Dyck, C. Uher, and M. G. Kanatzidis, J. Appl. Phys. **100**, 123704 (2006).

[8] S. H. Tessmer, D. J. Van Harlingen, and J. W. Lyding, Rev. Sci. Instrum. **65**, 2855 (1994).

[9] Diffuse reflectance spectroscopy measurements of β-$K_2Bi_8Se_{13}$ at room temperature suggested an apparent band gap of ~0.59 eV (Ref. 2). The key difference between the optical and tunneling measurements of the band gap is that optical measurements are sensitive to wave vector **k** and optical matrix element connecting the valence and conduction band states. In contrast, the tunneling measurements are sensitive to the matrix element between the states of the system and the tip. This difference may be the reason for observed difference in the values of the band gap seen in tunneling and reflectance spectroscopy measurement.

[10] P. Soven, Phys. Rev. **156**, 809 (1967).

[11] B. L. Gyorffy, Phys. Rev. B **5**, 2382 (1972).

[12] J. P. Perdew, K. Burke, and M. Ernzerhof, Phys. Rev. Lett. **77**, 3865 (1996).

[13] P. E. Blöchl, Phys. Rev. B **50**, 17953 (1994).

[14] G. Kresse and D. Joubert, Phys. Rev. B **59**, 1758 (1999).
[15] G. Kresse and J. Hafner, Phys. Rev. B **47**, 558 (1993).
[16] G. Kresse and J. Furthmüller, Phys. Rev. B **54**, 11169 (1996).
[17] G. Kresse and J. Furthmüller, Comput. Mater. Sci. **6**, 15 (1996).
[18] H. J. Monkhorst and J. D. Pack, Phys. Rev. B **13**, 5188 (1976).
[19] W. G. Aulber, L. Jönsson, and J. W. Wilkins, Solid State Phys. **54**, 1 (2000).
[20] K. Hoang, S. D. Mahanti, J. R. Salvador, and M. G. Kanatzidis, Phys. Rev. Lett. **99**, 156403 (2007).
[21] K. Hoang and S. D. Mahanti, Phys. Rev. B **77**, 205107 (2008).
[22] Y. Pan, F. Inam, M. Zhang, and D. A. Drabold, Phys. Rev. Lett. **100**, 206403 (2008).
[23] S. J. L. Billinge and I. Levin, Science **316**, 561 (2007).
[24] T. J. McCarthy, S. P. Ngeyi, J. H. Liao, D. C. DeGroot, T. Hogan, C. R. Kannewurf, and M. G. Kanatzidis, Chem. Mater. **5**, 331 (1993).